Monte Carlo Study of the Effect of Pressure on Hydrophobic Association

Vilia Ann Payne, Nobuyuki Matubayasi, Lynne Reed Murphy, and Ronald M. Levy

Department of Chemistry, Wright & Rieman Laboratories, Rutgers University, Piscataway, New Jersey 08855-0939

The Journal of
Physical Chemistry B®

Reprinted from
Volume 101, Number 11, Pages 2054–2060

Monte Carlo Study of the Effect of Pressure on Hydrophobic Association

Vilia Ann Payne, Nobuyuki Matubayasi,† Lynne Reed Murphy, and Ronald M. Levy*

Department of Chemistry, Wright & Rieman Laboratories, Rutgers University, Piscataway, New Jersey 08855-0939

Received: September 26, 1996; In Final Form: December 23, 1996[⊗]

This paper describes a series of simulations using pressure as a tool to study the hydrophobic interaction between two simple solutes. The change in the free energy of association ($\Delta\Delta G_r$) of the solutes as a function of pressure is expressed in terms of the change in partial molar volume ($\Delta V°$) and the change in isothermal compressibility ($\Delta\kappa°$) of the system. At 30 °C, $\Delta V°$ is found to be -7.4 ± 1.1 mL mol^{-1}, and $\Delta\kappa°$ is found to be $(-1.4 \pm 0.3) \times 10^{-3}$ mL mol^{-1} bar^{-1}. The two effects are in opposition to each other: The volume term tends to favor solute association, while the compressibility term favors dissociation. The volume term is the dominant one in determining $\Delta\Delta G_r$ at moderate pressures. At higher pressures (above 5 kbar), the opposing effect becomes dominant. A new analysis of experimental data concerning pressure-dependent effects in the association constants for a series of carboxylic acids (Suzuki, K.; Taniguchi, Y.; Watanabe, T. *J. Phys. Chem.* **1973**, *77*, 1918−1922) lends support for these conclusions. The applicability of these results to understanding protein stability is discussed. The compressibility change provides an explanation for the pressure-induced denaturation of some proteins.

I. Introduction

Hydrophobic interactions are often proposed to be the engine that drives proteins to fold into a molten globule state and exclude water from the interior of the protein, while hydrogen bonds and packing effects are attributed as the specific interactions that create the native state.[1,2] Researchers have traditionally used the transfer of hydrocarbons from water to a nonpolar environment as a simplifying model of protein folding.[3] In his review on this subject, Kauzmann points out that although the hydrocarbon model is consistent for the entropy and enthalpy changes caused by thermal denaturation, it fails for the volume changes (ΔV) of pressure denaturation.[4] At low pressures, the ΔV of protein unfolding is small and positive but becomes negative at pressures above 1−2 kbar. For the transfer of nonpolar solutes to an aqueous environment, ΔV is negative at low pressures but becomes positive at pressures above 1−2 kbar.[4−6] We note that physical chemists usually reserve the term "high pressure" for pressures in the range 10−100 kbar, but for biomolecules, pressures in the range 1−10 kbar are considered high and cause measurable effects such as protein denaturation.[7−9] For the purposes of this paper, pressures greater than 1 kbar will be considered high.

Protein folding at ambient pressure is accompanied by only small volume changes,[6,10] but at high pressures the partial molar volume of the denatured protein decreases. This is true for a variety of proteins.[6,11,12] Negative volume changes upon denaturation, sometimes reaching as much as −100 mL/mol,[11] drive many proteins to denature at pressures of several kbar. These volume changes typically correspond to 2% or less of the volume of the protein molecule.[13] Weber and Drickamer describe this process as the penetration of water into the protein structure.[10] They suggest that it is unlikely that the volume decrease could be due to changes in ionization of ionic residues, and the most common explanation has been that pressure denaturation is driven by inefficiency of packing within the protein interior. In other words, pressure denaturation is driven by the presence of internal cavities in the protein, which disappear during unfolding. The discussion of packing defects is made difficult by disagreement about the assignment of residue volumes.[2] However, recent articles have presented a strong case that protein interiors are packed more efficiently than previously thought.[6,14]

For any reaction, a positive volume of reaction will decrease the extent of reaction with increasing pressure, while a negative volume of reaction will increase the extent of reaction with increasing pressure. This statement is simply a consequence of Le Chatelier's principle. At low pressures, the volume change (ΔV) can be approximated by the volume change at 1 bar ($\Delta V°$). However, at the high pressures at which proteins denature, the second-order effect of compressibility must be considered. At these pressures, ΔV can no longer be predicted from knowledge of $\Delta V°$ alone. A positive compressibility change indicates that the reaction products are more compressible than the reactants and favors a greater extent of reaction at higher pressure.

A report from this group on the high-pressure simulation of solvated protein shows that the application of high pressure results in significant changes in the hydration layer of the protein.[15] Compressibility measurements have been used to detect the conformational state of a protein.[16−18] Compressibility appears to be positively correlated with the hydrophobicity of a series of globular proteins.[18] On the other hand, electrostriction of water around ionic groups at normal pressure causes the water to behave like water under high pressure, and to a lesser extent the same is true of water solvating polar groups.[18] It is reasonable, therefore, to look for the greatest possibility of compression with pressure in the water associated with hydrophobic groups, which is less tightly packed at normal pressures than the water solvating ionic or polar groups.

To our knowledge, no computational study has been reported calculating the volume change and compressibility change due to hydrophobic association. An objective of this paper is to calculate these quantities for the association reaction of two hydrophobic solutes. We then try to relate those results to the understanding of pressure effects on protein stability. Simula-

* To whom correspondence should be addressed.
† Present address: Institute for Chemical Research, Kyoto University, Uji, Kyoto, 611, Japan.
⊗ Abstract published in *Advance ACS Abstracts,* February 15, 1997.

S1089-5647(96)02977-X CCC: $14.00

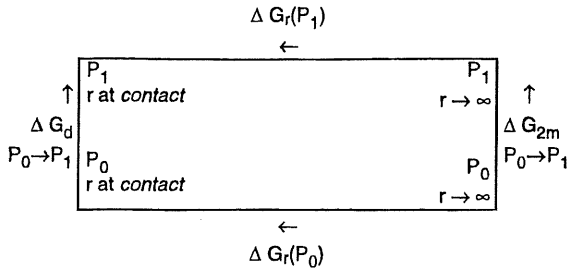

Figure 1. Thermodynamic cycle for the association–dissociation reaction of two solutes at two different pressures (P_0 and P_1) is displayed. The governing equation is $\Delta\Delta G_r = \Delta G_r(P_1) - \Delta G_r(P_0) = \Delta G_d(P_0 \rightarrow P_1) - \Delta G_{2m}(P_0 \rightarrow P_1)$, which expresses the change with pressure in the free energy of reaction when going from the monomer state (2m) to the dimer state (d).

tions of the potential of mean force of two model methanes in aqueous solution at 30 °C are carried out for seven different pressures ranging from 1 bar to 7 kbar. It is demonstrated that for this model system, the volume of association ($\Delta V°$) is negative and that this effect is dominant at moderate pressures, but that an opposite trend produced by the isothermal compressibility change ($\Delta\kappa°$) becomes dominant at greater pressures. The crossover occurs in the pressure region around 5 kbar. This association corresponds to the partial removal of the solutes from the aqueous environment. The observed behavior is contrary to the experimental behavior of the transfer of small nonpolar solutes from the liquid hydrocarbon phase to water,[4] but it is consistent with the pressure dependence of the volume changes associated with protein unfolding: At lower pressures ΔV is positive, but at higher pressures it is negative.

II. Theoretical Background

Using X to represent a dilute species in aqueous solution, the association of X to form a dimer X_2 can be expressed:

$$X(aq) + X(aq) \rightleftarrows X_2(aq) \tag{1}$$

By use of d for the dimer state and 2m for the separated monomer state, the free energy of association at two pressures P_0 and P_1 is denoted by

$$\Delta G_r(P_0) = G_d - G_{2m} \quad \text{(at pressure } P_0\text{)} \tag{2}$$

$$\Delta G_r(P_1) = G_d - G_{2m} \quad \text{(at pressure } P_1\text{)} \tag{3}$$

and the change in ΔG_r upon changing the pressure from P_0 to P_1 is then written

$$\Delta\Delta G_r = \Delta G_r(P_1) - \Delta G_r(P_0) \tag{4}$$

Figure 1 shows the thermodynamic cycle for this process.

The free energy of a substance at P_1 can be expressed in terms of the free energy at P_0 in the following manner,[19] where V is the volume:

$$G(P_1) = G(P_0) + \int_{P_0}^{P_1} V\,dP \tag{5}$$

In general, the analytical expression for V in terms of P is unknown. However, the equation may be rewritten as a Taylor expansion about the point P_0, where $\Delta P = P_1 - P_0$ and the superscript ° denotes the quantity at P_0:

$$\Delta G(P_0 \rightarrow P_1) = G(P_1) - G(P_0) = (\Delta P)V° + \frac{1}{2}(\Delta P)^2\frac{dV°}{dP} + \frac{1}{6}(\Delta P)^3\frac{d^2V°}{dP^2} + \ldots \tag{6}$$

By replacment of G with ΔG_r, the free energy of association, and truncation of the expansion after the quadratic term, the following equation is obtained:

$$\Delta\Delta G_r = (\Delta P)(\Delta V°) + \frac{1}{2}(\Delta P)^2\frac{d(\Delta V°)}{dP} \tag{7}$$

$\Delta V°$ is the change in volume for the association reaction at P_0. An equivalent way to define $\Delta V°$ is $\Delta V_d° - 2\Delta V_m°$, where $\Delta V_d°$ and $\Delta V_m°$ are the excess volumes at P_0 for a dimer and a single monomer. The excess volume for the solute is the change in volume of the system on addition of the solute at an arbitrarily chosen fixed origin.[20]

The change in the excess volume with pressure, $d(\Delta V°)/dP$, is not measured directly. Instead, it is the excess compressibility $\Delta\kappa°$ that is experimentally determined. Now the relationship between $d(\Delta V°)/dP$ and $\Delta\kappa°$ will be derived. The effect of pressure on the associated and dissociated states can be characterized by the isothermal (constant temperature T) compressibility of each state

$$\kappa = \frac{-1}{V}\left(\frac{\partial V}{\partial P}\right)_T \tag{8}$$

This quantity is always positive for a given substance and has units of inverse pressure. Let N be the number of dimers in solution volume V_d formed from $2N$ monomers in solution volume V_{2m}. The change in compressibility for the association reaction is defined as the limiting value of the slope of the change in compressibility with dimer concentration as the dimer concentration goes to zero[21]:

$$\Delta\kappa° = \lim_{C_d \rightarrow 0}\frac{1}{C_d}(\kappa_d - \kappa_{2m}) = \lim_{C_d \rightarrow 0}\frac{1}{C_d}\left[\frac{-1}{V_d}\left(\frac{\partial V_d}{\partial P}\right)_T - \frac{-1}{V_{2m}}\left(\frac{\partial V_{2m}}{\partial P}\right)_T\right] \tag{9}$$

where C_d is N/V_d, the concentration of the dimer. The partial molar quantity $\Delta\kappa°$ is thus rigorously defined at infinite dilution. By use of the substitution $V_d = N\Delta V° + V_{2m}$, $\Delta\kappa°$ may be rewritten as

$$\Delta\kappa° = -\Delta V°\kappa_o - \left(\frac{\partial\Delta V°}{\partial P}\right)_T \tag{10}$$

At infinite dilution, the total volume and total compressibility of either the monomer or dimer solution may be replaced with the volume V_o and compressibility κ_o of pure water. Note that $\Delta\kappa°$ remains nonzero at infinite dilution. C_d has units of mol mL^{-1}, so $\Delta\kappa°$ has units of mL mol^{-1} bar^{-1}.

Also, note that it is $(\partial\Delta V°/\partial P)_T$ and not $\Delta\kappa°$ that actually enters into the quadratic term of eq 7 and thus determines the effect of pressure on $\Delta\Delta G_r$. The sign of $(\partial\Delta V°/\partial P)_T$ may be either positive or negative, depending on whether the application of pressure drives the reaction backward or forward, respectively. Although $\Delta\kappa°$ is more commonly discussed, since it is the experimental observable, a clearer understanding of the effect of pressure on a given reaction will be attained after using $\Delta\kappa°$ to extract $(\partial\Delta V°/\partial P)_T$ from eq 10.

We have shown that $\Delta\Delta G_r$ can be decomposed into terms related to the change in volume and compressibility due to the reaction. In turn, $\Delta\Delta G_r$ is directly calculable from the potential of mean force (PMF) between the two solutes as determined from Monte Carlo simulations. In this case, the interaction between the two solutes is the pairwise Lennard-Jones potential, which is treated the same at all pressures. It is possible to

separate the solute–solute contribution to the PMF from the remaining solute–solvent plus solvent–solvent contribution and thus determine their relative contributions to $\Delta\Delta G_r$.

III. Methodology

The Monte Carlo (MC) simulations included 215 TIP4P model waters and two hydrophobic solutes assigned the Lennard-Jones parameters for methane of $\sigma_{SS} = 3.73$ Å, $\epsilon_{SS} = 0.2931$ kcal/mol, $\sigma_{SW} = 3.4475$ Å, and $\epsilon_{SW} = 0.2134$ kcal/mol, where the subscript S refers to the solute and W refers to the water oxygen site.[22,23] The positions of the solutes were fixed, but the solvent molecules were allowed to move.

The simulations employed preferential sampling, periodic boundary conditions, and an 8.5 Å spherical cutoff for force evaluation. The pressure was controlled by varying the volume. Consequently, the volume of the simulation cell was selected to give the desired pressure according to standard tables.[24] This procedure is acceptable,[25] since TIP4P water and experimental water show a similar pressure–volume dependence in the pressure regime considered in this paper.[26–29]

The potential of mean force at each pressure was calculated by the thermodynamic perturbation method.[30,31] After an initial equilibration of 129 million MC steps at each pressure, the evaluation took place in 0.2 Å increments for the solute–solute separation r, covering a distance from 2.4 to 8.4 Å. At each interval, the system was equilibrated for 10 million MC steps, and data were collected over 43 million MC steps. The free energy difference (FED) during each interval was calculated between r and $r + 0.1$ Å and between r and $r - 0.1$ Å.

The FED between reference state i and perturbed state j in the *NVT* ensemble is defined[30,31]

$$\Delta A = A_j - A_i = -k_b T \ln \langle \exp(-\beta(E_j - E_i)) \rangle_i \quad (11)$$

where k_b is the Boltzmann constant, β is $1/(k_b T)$, and E is potential energy. The simulations have been performed in the *NVT* ensemble rather than in the *NPT* ensemble to improve computational efficiency. However, the equations and results are reported using pressure rather than density (ρ) to simplify the analysis. It is a principle of thermodynamics that $\Delta A(\rho) = \Delta G(P(\rho))$ and that the relevant equations are equivalent in each ensemble.[32] This statement is equivalent to the observation that equilibrium constants are independent of the ensemble. Of course, it does not imply that $\Delta A(\rho) = \Delta G(\rho)$.

A simple estimate of the error associated with each FED calculation was obtained. The data at each window were divided into 200 sections and the FED calculated for each. A standard deviation of the mean calculated from the combined data was used as the error on the FED. Then the estimated error for each data point in the PMF was taken as the square root of the sum of squares of the errors for the FED values used to calculate that point. The error estimate for each PMF therefore represents a standard deviation of the mean value calculated during the simulation.

The Monte Carlo simulations discussed in this paper were performed on HP 735 RISC workstations. The two unknown quantities $\Delta V°$ and $d(\Delta V°)/dP$ were evaluated through a curve-fitting procedure based on eq 7. The KaleidaGraph general curve-fitting procedure used the Levenberg–Marquardt algorithm[33] for an equation of the form $y = ax + (1/2)bx^2$. Different initial estimates for the two unknown quantities a and b made no difference in the results. Then $\Delta\kappa°$ was evaluated from eq 10 using a value for k_o of 5.0×10^{-5} bar^{-1}.[27,32]

IV. Results and Discussion

The PMF curves computed at four different pressures (1 bar, 1 kbar, 5 kbar, and 7 kbar) at 30 °C are displayed in Figure 2.

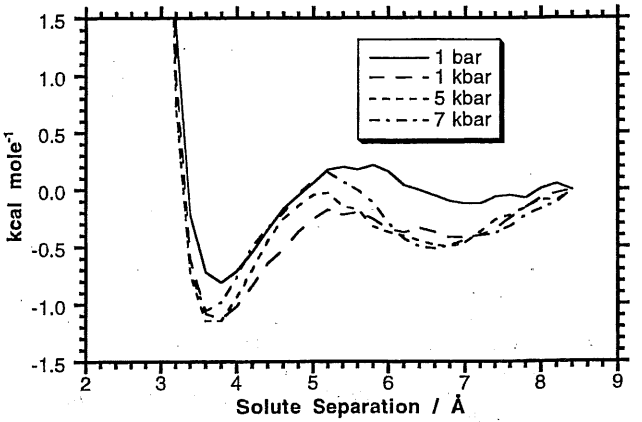

Figure 2. Potential of mean force curves at 1 bar, 1 kbar, 5 kbar, and 7 kbar are shown. The contributions at intermediate values of the pressure are omitted for visual clarity. Data are normalized to be zero at the potential cutoff (8.5 Å).

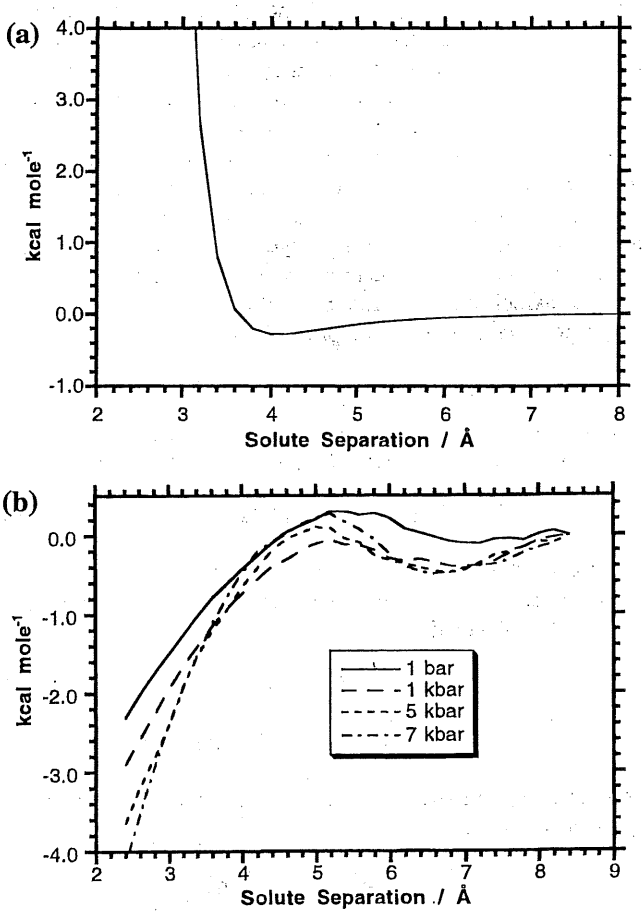

Figure 3. (a) Solute–solute contribution to the potential of mean force is shown. For the potential function used here, it is the same at all temperatures and pressures. (b) Indirect (solute–solvent plus solvent–solvent) contributions to the potential of mean force are shown at 1 bar, 1 kbar, 5 kbar, and 7 kbar.

The application of high-pressure deepens the potential well observed at 3.8 Å and shifts it to slightly shorter distances. A second shallow well, which is commonly attributed to the solvent-separated pair,[34] appears to occur between 6 and 7 Å. The high-pressure curves remain below the 1 bar curve over the entire distance, except for the 7 kbar curve.

For a potential function of this type, the solute–solute (direct) contribution to the PMF (Figure 3a) can be separated from the solute–solvent plus solvent–solvent (indirect) contributions (Figure 3b). The former contribution is the same at all temperatures and pressures and can be analytically calculated

TABLE 1: Simulation Results for the Change in the Free Energy of Association ($\Delta\Delta G_r$) Due to the Change in Pressure (ΔP)

ΔP bar	$\Delta\Delta G_r$ mL bar mol^{-1}	% error for $\Delta\Delta G_r$	$\Delta\Delta G_r$ kcal mol^{-1}
0	0	2.9	0
999	−131 26	2.3	−0.314
1999	−123 64	2.5	−0.296
2999	−131 65	2.3	−0.315
3999	−133 73	2.6	−0.320
4999	−138 75	2.8	−0.332
6999	−101 30	3.1	−0.242

from the Lennard-Jones potential. The minimum in the solute−solute potential well occurs at 4.0 Å, and the potential increases sharply at shorter distances. It is clear that when the solutes are less than 4.0 Å apart, the driving force to push them closer together is entirely due to the indirect contributions. The free energy minimum in the PMF at 3.8 Å is due to the superposition of this indirect contribution to the curve onto the direct contribution, which is increasingly repulsive at shorter distances.

The driving force for association in the overlap region where the solute−solute distance is less than 3.5 Å (see Figure 3b) is the size effect of cavity formation. The reversible work of formation of a cavity is a monotonically increasing function of the cavity size. In the immediate neighborhood of contact between the solutes, the presence of an attractive well in the PMF deeper than k_bT reflects the balance between the direct solute−solute forces and the indirect effect on the solutes of the interactions among the solvents. This is the signature of the hydrophobic interaction.

Although the first minimum seen in Figure 2 is determined by the balance between the direct and indirect contributions, the second minimum, which is due to the solvent-separated pair and occurs at solute−solute distances between 6 and 7 Å, is dominated by the indirect contribution. The position and depth of the second minimum is thought to be a characteristic of the hydrophobic interaction.[20,23,35−38] Figure 2 shows that the second minimum deepens faster with pressure than the first minimum. In other words, the equilibrium between the contact pair and the solvent-separated pair is shifted toward the latter. Thus, the role of the solvent-separated pair is more important in the hydrophobic interaction at higher pressures.

In recent years, a number of computational investigations have sought to quantify and interpret the hydrophobic interaction in terms of enthalpic and entropic components.[23,32,34,38−55] For simulations of aqueous methane, a major source of controversy has been the relative magnitudes of the free energy minima of the contact dimer and the solvent-separated dimer.[34,52] Interpretation of results is also necessarily complicated by the use of different water models and solute potential functions.[23,53] However, a consensus has developed that the association of methane at short distances (less than 5 Å) is driven by entropy.[23,38] The low solubility of hydrophobic gases such as methane near room temperature is also governed by the unfavorable entropy,[23,47] whereas the enthalpy of solvation is favorable but smaller in magnitude near room temperature. This entropic effect can be traced to the ordering of waters, especially the increase in strength and number[39,42,45] of hydrogen bonds primarily but not exclusively in the solvation shell.[45] An increase in the duration of hydrogen bonds[54,55] is also seen, demonstrating the correlation between dynamics and structure. By the association of two methanes and the coalescence of two hydration shells into one, water regains some of the lost entropy.

Results for $\Delta\Delta G_r$ at each pressure are reported in Table 1. The free energy difference between the value at 8.5 Å and the minimum in the potential well is taken as ΔG_r for each simulation. Then $\Delta\Delta G_r$ is taken as the difference between ΔG_r at that pressure and ΔG_r at 1 bar. Figure 4 shows the plot of $\Delta\Delta G_r$ versus ΔP at the seven pressures studied.

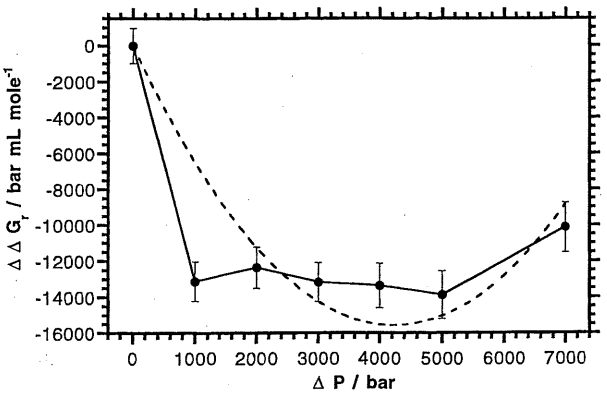

Figure 4. Plot of $\Delta\Delta G_r$ versus ΔP is shown as the solid line. Error bars are shown for each data point. The best fit based on eq 7 is shown as the dashed line.

Several options were tried in an attempt to find the best way to fit the data. In the end, a simple quadratic curve fit to eq 7 was found to give the results most suited to interpretation, as will be discussed further below. This curve fit gave a regression coefficient of 0.79 and is shown as a dashed line in Figure 4. The value for $\Delta V°$ was calculated to be -7.4 ± 1.1 mL mol^{-1}. For comparison, we note that the excess volume $\Delta V_m°$ for the methane monomer has been determined experimentally to be 36 mL mol^{-1} and calculated from simulations to be 35 mL mol^{-1}.[32] The value for $d(\Delta V°)/dP$ was calculated to be 0.001 75 mL mol^{-1} bar^{-1}, giving a value for $\Delta\kappa°$ of $(-1.4 \pm 0.3) \times 10^{-3}$ mL mol^{-1} bar^{-1}.

These results depend to some extent on the choice of normalization of the PMF curves: The curves were overlapped at the Lennard-Jones cutoff of 8.5 Å. To test the sensitivity of the extracted parameters to the normalization, another fit was performed based on a normalization of each PMF using the mean of the three points between 8.0 and 8.5 Å. The results are the same within error bars.

From Figure 4 it is apparent that the quadratic fit fails to reproduce the steep descent of $\Delta\Delta G_r$ between 1 bar and 1 kbar. The relatively poor regression coefficient of the fit can be attributed to this cause. Several options were tried in order to improve the fit. The results for the quadratic fit described above are quite stable for a variety of initial conditions. The use of interpolation or smoothing techniques was of no value. A three-parameter fit adding the term involving $d^2(\Delta V°)/dP^2$ shown in eq 6 produced a higher regression coefficient but also added an inflection point around 6 kbar, which is contrary to the shape of the data. An expansion to many terms of eq 6 is probably required to reproduce the data adequately, although the higher derivatives are unlikely to be experimentally determinable and contain little information that can be interpreted with a simple physical picture.

On the other hand, conclusions of value can be obtained from the results of the quadratic fit. First of all, it must be remembered that discussing the effect of pressure in terms of volume and compressibility changes is an approximation based on the neglect of higher derivatives. In any case, the main conclusion is that the volume change and compressibility change have opposing effects on $\Delta\Delta G_r$. This idea is illustrated dramatically in Figure 5, where the linear term and quadratic term of eq 7 are graphed together. At moderate pressures, the linear term arising from the volume change is dominant, and $\Delta\Delta G_r$ becomes more negative as pressure increases. At

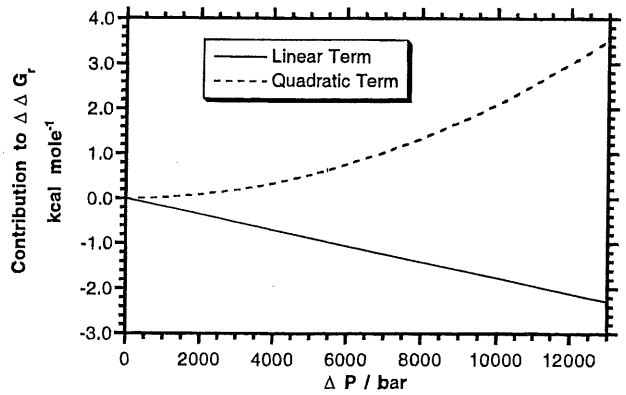

Figure 5. Values of $\Delta V°$ and $d(\Delta V°)/dP$ calculated from the curve fit shown in Figure 4 are used to break eq 7 down into linear (first term) and quadratic (second term) contributions. The quadratic term becomes dominant at pressures above 5 kbar.

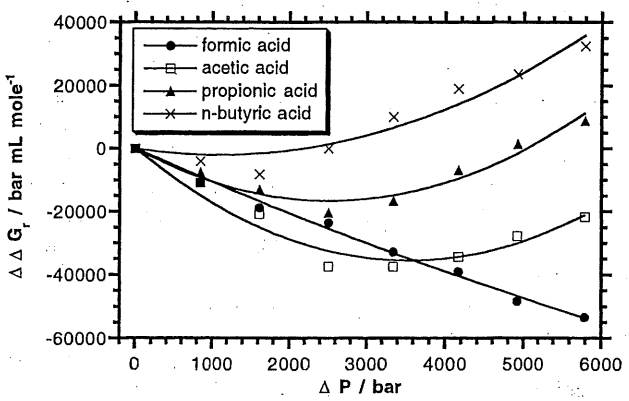

Figure 6. Plot of $\Delta\Delta G_r$ versus ΔP based on the data in ref 57 is shown for four carboxylic acids at 30 °C. The lines through the data points are the best curve fits based on eq 7.

pressures greater than 5 kbar, the quadratic term arising from the compressibility change becomes dominant, and $\Delta\Delta G_r$ increases as pressure increases. Figure 4 also shows that these two domains are separated by an almost flat region between 1 and 5 kbar. In this intermediate domain, increasing the pressure has little effect on $\Delta\Delta G_r$.

There are few experimental studies on model systems that provide direct information about pressure effects on hydrophobic association. Ben-Naim[56] has developed a model for hydrophobic association based on analyzing the difference in solubilities between methane and ethane. In this model, ethane approximates the properties of the associated methane dimer. According to Ben-Naim's analysis, the sign of $\Delta V°$ is negative, in agreement with the simulations reported here. A different model for pressure effects on hydrophobic association was studied by Suzuki, Taniguchi, and Watanabe.[57] In this paper, the effect of pressure on the dimer dissociation constants (K_D) of the first four carboxylic acids (formic, acetic, propionic, and *n*-butyric) at 30 °C is determined. Their experimental results are shown as the data points in Figure 6 after conversion to the units used in this paper.

The authors make no mention of any quadratic effects due to the change in the compressibility of the solution upon dimer dissociation when analyzing their data. Instead, they attribute the minimum in dimer concentration plotted against pressure to the sum of two effects, hydrogen bonding and hydrophobic association, apparently considering each to exhibit strictly linear behavior. By the assumption that the formic acid dimer has no hydrophobic association, the negative slope of $\Delta\Delta G_r$ versus ΔP for formic acid is used to conclude that hydrogen bonding contributes a negative component to $\Delta V°$. Because the plots

TABLE 2: Results of Curve Fits Based on the Data in Ref 57 for Four Carboxylic Acids

acid	$\Delta V°$ mL mol^{-1}	$d(\Delta V°)/dP$ 10^{-3} mL mol^{-1} bar^{-1}	$\Delta\kappa°$ 10^{-3} mL mol^{-1} bar^{-1}
formic	-11 ± 1	0.5 ± 0.3	0.05 ± 0.04
acetic	-20 ± 2	5.7 ± 0.6	-4.7 ± 1.0
propionic	-13 ± 1	5.2 ± 0.5	-4.6 ± 0.8
n-butyric	-3.7 ± 1.7	3.4 ± 0.7	-3.2 ± 2.1

of the other carboxylic acids show inversion points, they conclude that hydrophobic association contributes a positive component to $\Delta V°$, in disagreement with our results, as well as in disagreement with Ben-Naim's analysis.[56] However, the sum of two linear effects must be a linear effect and cannot lead to an inversion point. It is necessary to include quadratic effects due to the difference in compressibilities between the reactant and product solutions in order to explain the experimental data in Figure 6.

In Figure 6, a new analysis of the data in ref 57 is presented. By use of the K_D provided by the experiments, $\Delta\Delta G_r$ was calculated for the association of two acid monomers and plotted versus ΔP. The $\Delta\Delta G_r$ for formic acid exhibits linear behavior up to 6 kbar, while the other three acids show quadratic behavior similar to that seen in Figure 4. The minima in $\Delta\Delta G_r$ appear at lower pressures and grow more shallow as the acid size increases.

Table 2 presents the results of curve fits based on eq 7 for the four acids. The quantity $\Delta\kappa°$ is an order of magnitude smaller for formic acid than for the other three acids. It seems clear that in order to create an observable quadratic effect at pressures of several kbar, $\Delta\kappa°$ must be on the order of 10^{-3} mL mol^{-1} bar^{-1}. Assuming that formic acid does not exhibit hydrophobic association and that the other acids do, then the data indicate that the compressibility change due to hydrophobic association creates the quadratic effect in these compounds, driving the dimers apart as the pressure increases. The results of the data analysis presented in Figure 6 and Table 2 provide evidence to support our main conclusions: The compressibility change for acetic, propionic, and *n*-butyric acid, which can be attributed to the hydrophobic effect, has a magnitude and sign sufficient to drive the solutes apart at pressures of several kbar.

The shallower minima seen in Figure 6 as the acid size increases can be attributed to a $\Delta V°$ that decreases in magnitude. This finding is inconsistent with a strictly additive model of the hydrophobic interaction, in which case the addition of methyl groups would increase the magnitude of the linear term, $\Delta V°$, proportional to the number of substituent methyl groups. In any case, the structures of the dimers are not known, and the possibility of interactions between hydrophilic and hydrophobic portions of these acids upon dimerization complicates a more detailed interpretation of the data.

V. Conclusions

The hydrophobic interaction between two simple solutes has been investigated by studying the effect of high pressure on the potential of mean force. The pressure-induced change in the free energy of solute association has been expressed in terms of the change in reaction volume and isothermal compressibility. The volume of association is clearly negative at 30 °C, and this effect is dominant in regions of moderate pressure. In this pressure domain, increasing pressure serves to drive hydrophobic solutes together. At higher pressures of several kbar, the quadratic term due to the compressibility change becomes dominant. In this domain, increasing the pressure serves to decrease the attraction between the solutes.

In a series of papers,[58-60] Wallqvist explored aspects of the hydrophobic interaction using a concentrated solution of methane-like particles. His results show that at low pressures, the solution separates into a methane-rich phase and a water-rich phase. At high pressures, the solution structure is quite different; Methane monomers or small methane clusters are solvated in clathrate-type water structures. His findings are thus consistent with our conclusions that the application of pressure can disperse methane clusters in water.

These results provide a possible explanation for why native states of many proteins undergo pressure-induced denaturation at pressures in the range 2−10 kbar. The natural hypothesis is that proteins are packed more efficiently than generally assumed. In fact, the interior of the native protein is packed more efficiently than water can pack around the unfolded protein. The first-order effect of unfolding is a volume increase, leading to positive volumes of unfolding at moderate pressures. At higher pressures, the compressibility of the solution components becomes important. The solution containing the unfolded protein is more compressible than the solution containing the native state. This quadratic effect overcomes the linear effect at pressures of several kbar, and the protein unfolds.

Whether hydrophobic, ionic, or polar effects are the cause of pressure-induced protein denaturation has been the subject of debate for a long time. Our results support the hypothesis that hydrophobic forces drive the denaturation. Consider the following thought experiment. Two groups in the interior of a protein are bound through a salt bridge, if they are ionic groups, or hydrophobic association, if they are nonpolar groups. When denaturation occurs, the contact is broken and the groups are solvated by water instead. At low pressures, water around the ionic groups is already much denser than bulk water because of electrostriction. At high pressures, therefore, the greatest point of resistance to further compaction is near ionic groups. A similar line of reasoning follows for polar groups. Therefore, the contribution of protein unfolding to ΔV at a given pressure differs less from ΔV° at atmospheric pressure for ionic or polar groups than for nonpolar groups. Thus, pressure-induced protein denaturation is attributed to compressibility changes (quadratic effects) associated with the solvation of hydrophobic groups that are buried in the native structure of the folded protein. The idea that water is more compressible around hydrophobic solutes than around polar and ionic solutes or bulk water is supported by experimental evidence[61] and simulations of proteins.[15,62] As a note of caution, it should be added that we have recently shown through a statistical mechanical analysis of the hydration shell model[32] that the experimentally determined compressibility change for a hydrophobic solute in water is not simply proportional to the response of the solvent within the first hydration shell.

The mechanisms of protein folding and protein denaturation are much more complicated processes than the dimerization of a simple solute. Pathways of protein folding and unfolding can be proposed based on an analysis of various protein structures.[63,64] The irregular shape of the protein, which contains deep grooves and crevices, has a measurable effect on the packing efficiency at the surface. However, since pressure-induced unfolding appears to be a universal phenomenon, it is reasonable to assume there is a simple underlying explanation.

A remaining question is why these results do not reflect the experimental behavior of the transfer of small hydrocarbon solutes between water and nonpolar liquids. Although the hydrocarbon model has had success in explaining the temperature dependence of protein denaturation,[65] it is still questionable if the protein interior is much like a liquid hydrocarbon at all.[4,66] On the other hand, a qualitative difference has been postulated to exist between the pairwise hydrophobic interaction between two isolated solutes and the bulk hydrophobic interaction in a liquid hydrocarbon.[52] The liquid hydrocarbon phase may thus be unlike either a protein interior or the pairwise hydrophobic interaction. In this case, the transfer of model solutes between a liquid hydrocarbon phase and water is not a good model for protein denaturation.

Acknowledgment. This work was supported by the NIH (GM-30580 and GM-55210) and by the Rutgers University Center for Advanced Food Technology. V.A.P. acknowledges support from an NIH postdoctoral National Research Service Award (GM-17861). We thank Gabriela Del Buono and Francisco Figueirido for useful comments on the manuscript. R.M.L. thanks Y. Taniguchi for bringing ref 57 to our attention.

References and Notes

(1) Hunt, N. G.; Gregoret, L. M.; Cohen, F. E. *J. Mol. Biol.* **1994**, *241*, 214−225.
(2) Richards, F. M.; Lim, W. A. *Q. Rev. Biophys.* **1994**, *26*, 423−498.
(3) Zipp, A.; Kauzmann, W. *Biochemistry* **1973**, *12*, 4217−4228.
(4) Kauzmann, W. *Nature* **1987**, *325*, 763−764.
(5) Scheraga, H. A. *ACS Symp. Ser.* **1994**, *568*, 360−370.
(6) Harpaz, Y.; Gerstein, M.; Chothia, C. *Structure* **1994**, *2*, 641−649.
(7) Jonas, J.; Jonas, A. *Annu. Rev. Biophys. Biomol. Struct.* **1994**, *23*, 287−318.
(8) Peng, X.; Jonas, J.; Silva, J. L. *Biochemistry* **1994**, *33*, 8323−8329.
(9) Zhang, J.; Peng, X.; Jonas, A.; Jonas, J. *Biochemistry* **1995**, *34*, 8631−8641.
(10) Weber, G.; Drickamer, H. G. *Q. Rev. Biophys.* **1983**, *16*, 89−112.
(11) Royer, C. A.; Hinck, A. P.; Loh, S. N.; Prehoda, K. E.; Peng, X.; Jonas, J.; Markley, J. L. *Biochemistry* **1993**, *32*, 5222−5232.
(12) Samarasinghe, S. D.; Campbell, D. M.; Jonas, A.; Jonas, J. *Biochemistry* **1992**, *31*, 7773−7778.
(13) Mozhaev, V. V.; Heremans, K.; Frank, J.; Masson, P.; Balny, C. *Proteins: Struct. Funct. Genet.* **1996**, *24*, 81−91.
(14) Yee, D. P.; Chan, H. S.; Havel, T. F.; Dill, K. A. *J. Mol. Biol.* **1994**, *241*, 557−573.
(15) Kitchen, D. B.; Reed, L. H.; Levy, R. M. *Biochemistry* **1992**, *31*, 10083−10093.
(16) Chalikian, T. V.; Gindikin, V. S.; Breslauer, K. J. *J. Mol. Biol.* **1995**, *250*, 291−306.
(17) Chalikian, T. V.; Breslauer, K. J. *Proc. Natl. Acad. Sci. U.S.A.* **1996**, *93*, 1012−1014.
(18) Chalikian, T. V.; Sarvazyan, A. P.; Breslauer, K. J. *Biophysical Chemistry* **1994**, *51*, 89−109.
(19) Atkins, P. W. *Physical Chemistry*, 3rd ed.; W. H. Freeman and Company: New York, 1986.
(20) Ben-Naim, A. *Hydrophobic Interactions*; Plenum Press: New York, 1980.
(21) Note that the definition of the partial molar compressibility given in eq 9 is different from the one given in our previous paper [15]. In the latter, the translational contribution is excluded from the outset. The relationship between these two definitions is given in the appendix of [15].
(22) Jorgensen, W. L.; Madura, J. D.; Swenson, C. J. *J. Am. Chem. Soc.* **1984**, *106*, 6638−6646.
(23) Smith, D. E.; Haymet, A. D. J. *J. Chem. Phys.* **1993**, *98*, 6445−6454.
(24) Haar, L.; Gallagher, J. S.; Kell, G. S. *NBS/NRC Steam Tables*; Hemisphere: New York, 1984.
(25) It should be noted that the standard tables are calibrated for pure water and not for mixtures of water and hydrophobic solutes. Although the molar concentration of solute is small in these simulations, there may be an effect on the calibration of the density with pressure. This would affect the results quantitatively, but the qualitative conclusions would remain the same.
(26) Jorgensen, W. L.; Chandrasekhar, J.; Madura, J. D.; Impey, R. W.; Klein, M. L. *J. Chem. Phys.* **1983**, *79*, 926−935.
(27) Jorgensen, W. L.; Madura, J. D. *Mol. Phys.* **1985**, *56*, 1381−1392.
(28) Madura, J. D.; Pettitt, B. M.; Calef, D. F. *Mol. Phys.* **1988**, *64*, 325−336.
(29) Brodholt, J.; Wood, B. *Geochim. Cosmochim. Acta* **1990**, *54*, 2611−2616.
(30) Zwanzig, R. W. *J. Chem. Phys.* **1954**, *22*, 1420.
(31) Huston, S. E.; Rossky, P. J. *J. Phys. Chem.* **1989**, *93*, 7888−7895.
(32) Matubayasi, N.; Levy, R. M. *J. Phys. Chem.* **1996**, *100*, 2681−2688.

(33) Press, W. H.; Flannery, B. P.; Teukolsky, S. A.; Vetterling, W. T. *Numerical Recipes in C*; Cambridge University Press: New York, 1988.
(34) Dang, L. X. *J. Chem. Phys.* **1994**, *100*, 9032−9034.
(35) Pangali, C.; Rao, M.; Berne, B. J. *J. Chem. Phys.* **1979**, *71*, 2982−2990.
(36) Pangali, C.; Rao, M.; Berne, B. J. *J. Chem. Phys.* **1979**, *71*, 2975−2981.
(37) Pratt, L. R.; Chandler, D. *J. Chem. Phys.* **1977**, *67*, 3683−3704.
(38) Smith, D. E.; Zhang, L.; Haymet, A. D. J. *J. Am. Chem. Soc.* **1992**, *114*, 5875−5876.
(39) Guillot, B.; Guissani, Y.; Bratos, S. *J. Chem. Phys.* **1991**, *95*, 3643−3648.
(40) Guillot, B.; Guissani, Y. *J. Chem. Phys.* **1993**, *99*, 8075−8094.
(41) Head-Gordon, T. *J. Am. Chem. Soc.* **1995**, *117*, 501−507.
(42) Jorgensen, W. L.; Gao, J.; Ravimohan, C. *J. Phys. Chem.* **1985**, *89*, 3470−3473.
(43) Jorgensen, W. L.; Buckner, J. K.; Boudon, S.; Tirado-Rives, J. *J. Chem. Phys.* **1988**, *89*, 3742−3746.
(44) Kaminski, G.; Duffy, E. M.; Matsui, T.; Jorgensen, W. L. *J. Phys. Chem.* **1994**, *98*, 13077−13082.
(45) Matubayasi, N.; Reed, L. H.; Levy, R. M. *J. Phys. Chem.* **1994**, *98*, 10640−10649.
(46) Nagy, P. I.; Dunn, W. J., III; Nicholas, J. B. *J. Chem. Phys.* **1989**, *91*, 3707−3715.
(47) Silveston, R.; Kronberg, B. *J. Phys. Chem.* **1989**, *93*, 6241−6246.
(48) Skipper, N. T. *Chem. Phys. Lett.* **1993**, *207*, 424−429.
(49) Straatsma, T. P.; Berendsen, H. J. C.; Postma, J. P. M. *J. Chem. Phys.* **1986**, *85*, 6720−6727.
(50) Wallqvist, A.; Berne, B. J. *J. Phys. Chem.* **1995**, *99*, 2893−2899.
(51) Watanabe, K.; Andersen, H. C. *J. Phys. Chem.* **1986**, *90*, 795−802.
(52) Wood, R. H.; Thompson, P. T. *Proc. Natl. Acad. Sci. U.S.A.* **1990**, *87*, 946−949.
(53) Zeng, J.; Hush, N. S.; Reimers, J. R. *Chem. Phys. Lett.* **1993**, *206*, 318−322.
(54) Zichi, D. A.; Rossky, P. J. *J. Chem. Phys.* **1986**, *84*, 2814−2822.
(55) Zichi, D. A.; Rossky, P. J. *J. Chem. Phys.* **1986**, *84*, 2823−2826.
(56) Ben-Naim, A. *Hydrophobic Interactions*; Plenum Press: New York, 1980; p 211.
(57) Suzuki, K.; Taniguchi, Y.; Watanabe, T. *J. Phys. Chem.* **1973**, *77*, 1918−1922.
(58) Wallqvist, A. *Chem. Phys. Lett.* **1991**, *182*, 237−241.
(59) Wallqvist, A. *J. Phys. Chem.* **1991**, *95*, 8921−8927.
(60) Wallqvist, A. *J. Chem. Phys.* **1992**, *96*, 1655−1656.
(61) Gekko, K.; Noguchi, H. *Macromolecules* **1974**, *7*, 224−229.
(62) Gerstein, M.; Tsai, J.; Levitt, M. *J. Mol. Biol.* **1995**, *249*, 955−966.
(63) Sundaralingam, M.; Sekharudu, Y. C. *Science* **1989**, *244*, 1333−1337.
(64) Nicholls, A.; Sharp, K. A.; Honig, B. *Proteins: Struct. Funct. Genet.* **1991**, *11*, 281−296.
(65) Baldwin, R. L. *Proc. Natl. Acad. Sci. U.S.A.* **1986**, *83*, 8069−8072.
(66) Dill, K. A.; Bromberg, S.; Yue, K.; Fiebig, K. M.; Yee, D. P.; Thomas, P. D.; Chan, H. S. *Protein Sci.* **1995**, *4*, 561−602.